Journal of Magnetic Resonance Open 16–17 (2023) 100103

Contents lists available at ScienceDirect

Journal of Magnetic Resonance Open

journal homepage: www.sciencedirect.com/journal/journal-of-magnetic-resonance-open

Segmented solenoid RF coils for MRI of ex vivo brain samples at ultra-high field preclinical and clinical scanners

Daniel Papoti [a,b,*], Diego Szczupak [a], Luiz G.C. Santos [b], Khallil T. Chaim [c], Maria C.G. Otaduy [c], David J. Schaeffer [a], Edson L.G. Vidoto [d], Alberto Tannús [d], Afonso C. Silva [a]

[a] Department of Neurobiology, University of Pittsburgh, 3501 Fifth Avenue, 3058 Biomedical Science Tower 3, Pittsburgh, PA, 15261, United States of America
[b] Universidade Federal do ABC, Rua Arcturus, 03 – Jardim antares, São Bernardo do Campo, São Paulo, 09606-070, Brazil
[c] LIM44 - Instituto e Departamento de Radiologia, Faculdade de Medicina da Universidade de São Paulo, Travessa da R. Ovídio Pires de Campos, 75, São Paulo, São Paulo, 05403-010, Brazil
[d] Centro de Imagens e Espectroscopia por Ressonância Magnética - Instituto de Física de São Carlos, Universidade de São Paulo, Avenida Trabalhador São Carlense, 400, São Carlos, São Paulo, 13566-590, Brazil

ARTICLE INFO

Keywords:
RF coils
Magnetic resonance imaging
Ex vivo MRI
Solenoid coils

ABSTRACT

Magnetic resonance imaging (MRI) is a well-known and widespread imaging modality for neuroscience studies and the clinical diagnoses of neurological disorders, mainly due to its capability to visualize brain microstructures and quantify various metabolites. Additionally, its noninvasive nature makes possible the correlation of high-resolution MRI from ex vivo brain samples with histology, supporting the study of neurodegenerative disorders such as Alzheimer's or Parkinson's disease. However, the quality and resolution of ex vivo MRI highly depend on the availability of specialized radiofrequency coils with maximized filling factors for the different sizes and shapes of the samples to be studied. For instance, small, dedicated radiofrequency (RF) coils are not always commercially available in ultrahigh field whole-body MRI scanners. Even for ultrahigh field preclinical scanners, specific RF coils for *ex vivo* MRI are expensive and not always available. Here, we describe the design and construction of two RF coils based on the solenoid geometry for *ex vivo* MRI of human brain tissues in a 7T whole-body scanner and for *ex vivo* MRI of marmoset brain samples in a 9.4T preclinical scanner. We designed the 7T solenoid RF coil to maximize the filling factor of human brain samples conditioned on cassettes for histology, while the 9.4T solenoid was constructed to accommodate marmoset brain samples conditioned in 50 ml centrifuge tubes. Both solenoid designs operate in transceiver mode. The measured B_1^+ maps show a high level of homogeneity in the imaging volume of interest, with a high signal-to-noise ratio over the imaging volume. High-resolution (80 μm in plane, 500 μm slice thickness) images of human brain samples were acquired with the 7T solenoid, while marmoset brain samples were acquired with an isotropic resolution of 60 μm using the 9.4T solenoid coil.

1. Introduction

Magnetic resonance imaging (MRI) has become a primary imaging technique used in neuroscience, mainly due to its noninvasive characteristic and ability to visualize and quantify metabolites and brain microstructures. In addition, the ability to manipulate tissue contrast makes MRI an extensively used method to study ex vivo brain tissues [1–4]. Compared to in vivo MRI, *ex vivo* MRI allows the use of long acquisition times, providing images with very high spatial resolution and higher signal-to-noise ratio (SNR), free of motion artifacts and other physiological noise sources. For these reasons, imaging *postmortem* brain tissues weighted by different MRI contrasts, such as T_1, T_2, T_2*, susceptibility, proton density, diffusion tensor imaging (DTI), magnetization transfer imaging, and quantitative susceptibility mapping (QSM, [5]) have become widespread [3,6,7].

However, there are technical challenges in performing *ex vivo* MRI acquisitions, and in many circumstances, these acquisitions can be more complex than in vivo acquisitions [7]. For instance, in order to stop *postmortem* tissue degradation, it is necessary to use fixative chemicals such as formalin. Fixative solutions based on formaldehyde alter important tissue characteristics, such as the relaxation times T_1 and T_2 [2]. Another important challenge in performing *ex vivo* MRI is the

* Corresponding author.
E-mail address: daniel.papoti@ufabc.edu.br (D. Papoti).

https://doi.org/10.1016/j.jmro.2023.100103

Available online 8 March 2023

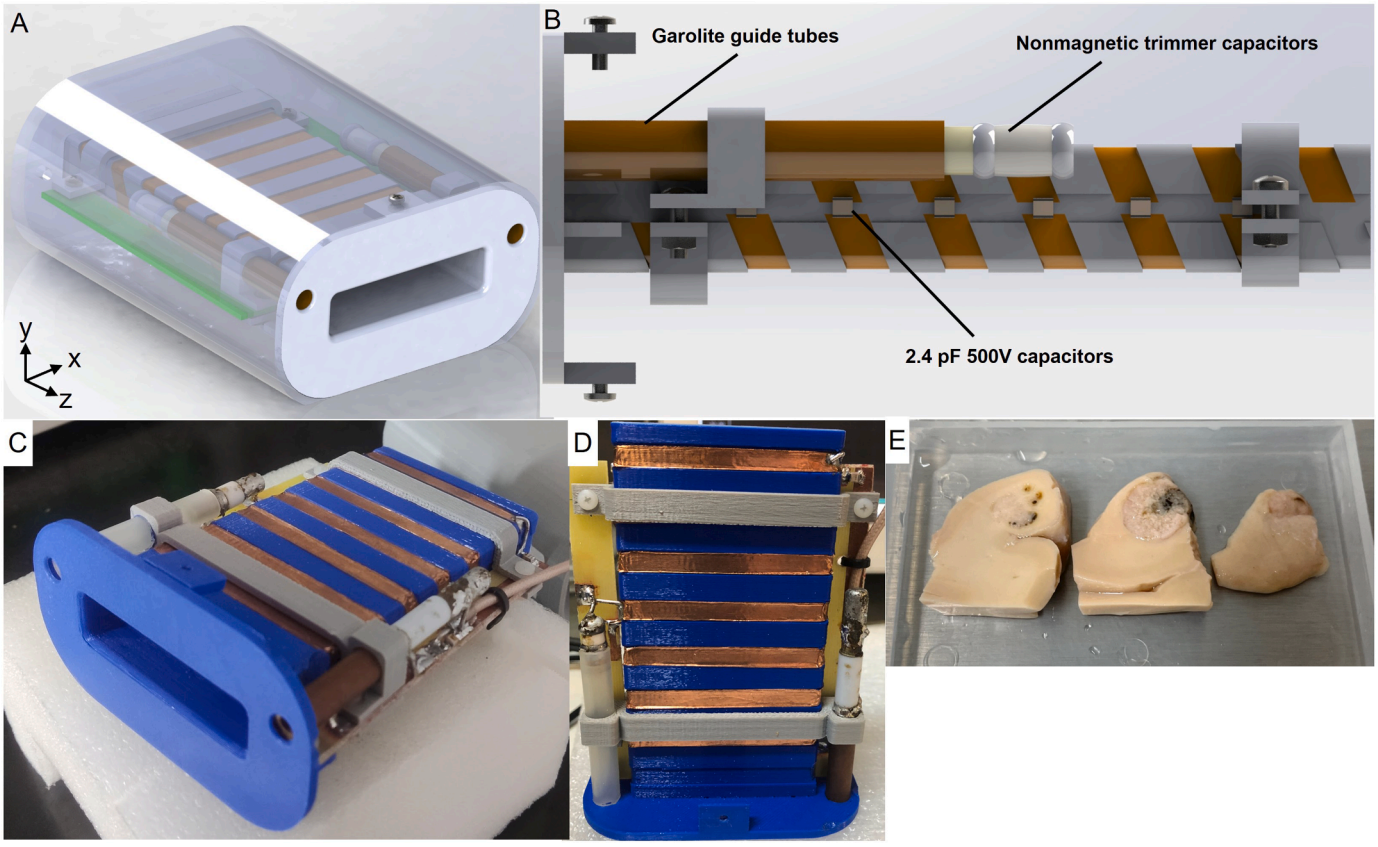

Fig. 1. (A) Rendered perspective view of the computer aided design file from the flat solenoid. (B) side view of the 3D file showing the 2.4 pF 500 V fixed capacitor. (C, D) Picture of the flat solenoid built using 6.3 mm width copper tape mounted on 3D-printed PLA support. The filling factor of this coil was maximized for brain tissues conditioned in histology cassettes measuring 40 × 30 × 6 mm (E).

presence of susceptibility artifacts [7]. When imaged in vivo, the brain is surrounded by cerebral spinal fluid (CSF) and other tissues that provide a relatively stable and homogeneous environment generally devoid of magnetic susceptibility. Once removed from the skull, however, regions with air-tissue interface cause severe susceptibility artifacts in the images. One strategy to mitigate this problem is using a fluid without hydrogen protons in its formulae, known as fomblin (Fomblin, Solvay USA, Inc). This fluid does not induce an MRI signal and has magnetic susceptibility similar to brain tissues [7].

From a technical side, especially at ultra-high magnetic field scanners (i.e.,$\geq$ 7 Tesla), dedicated radiofrequency (RF) coils with specific designs are fundamental to maximize the SNR in high-resolution acquisition. However, especially for ultra-high magnetic field (UHF) MRI scanners, there is a lack of commercially available RF coils with dedicated designs that maximize the filling factor (η) for each experiment to optimize the SNR, thus allowing acquisitions with higher spatial resolution. The filling factor is defined as the fraction of the coil volume (V_C) occupied by the volume of the sample (V_S), [8,9]:

$$\eta = \frac{V_S}{V_C} \tag{1}$$

For instance, most 7T clinical scanners are equipped with only one head coil, consisting of a quadrature Birdcage volume coil for transmission and 32 channels for receiving. The low filling factor provided by this coil for ex vivo sectioned brain tissue, such as the hippocampus or brain stem for pathology studies, compromises the SNR and spatial resolution of the experiments. The same scenario is relevant even for preclinical animal scanners. Most commercially available coils are designed for in vivo MRI of mice or rats and do not provide full SNR and maximum filling factor because the RF coils are not optimized for ex vivo samples. In addition, these RF coils are usually expensive and not affordable for many research centers where ex vivo studies are not the main research field.

The MRI phased array is a state-of-the-art coil design utilized in most MRI scanners [10]. This type of receive coil has the advantage of achieving high sensitivity over large imaging volumes by combining the signal of multiple distributed surface coil elements to cover a large field of view. Furthermore, phased array coils allow parallel imaging techniques, such as sensitivity encoding (SENSE) or generalized autocalibrating partial parallel acquisition (GRAPPA), reducing acquisition time. However, receive-only phased arrays require a separate transmit volume coil and have a high production cost due to the use of dedicated preamplifiers for each channel and the need to lay out each element carefully to achieve good preamplifier and geometric decoupling levels. Because axial access to the horizontal superconductor magnets is not a requirement for ex vivo MRI, it is possible to use the use the well-known solenoid design for the RF coil. Unlike phased arrays, the solenoid coil is a simple and affordable choice since its magnetic field produced (also called B_1 field) is homogenous and highly efficient in terms of SNR, as long as the primary coil axis is positioned perpendicular to the B_0 orientation.

In this work, we report the design, development, and characterization of two types of solenoid coils for *ex vivo* imaging at UHF scanners. One transmit/receive solenoid was designed for a 7T whole-body clinical scanner, with maximized filling factor for slices of human brain tissues conditioned in histological cassettes. The second solenoid coil, also designed as transmit/receive, was built for ex vivo MRI of marmoset brain samples conditioned in 50 mL centrifuge tubes at a 9.4T preclinical scanner.

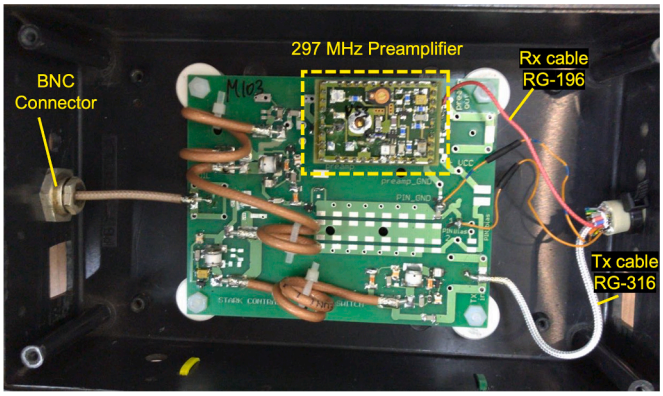

Fig. 2. 300 MHz TR Switch with BNC connector used to interface the flat solenoid coil with the 7T MRI scanner. Everything was assembled inside a plastic box, which can be used as an interface box for different designs of homebuilt RF coils.

2. Theory and methods

The solenoid coil design is optimal to provide homogeneous excitation with high sensitivity for nuclear magnetic resonance (NMR) experiments [11,12]. The fact that *ex vivo* MRI does not require axial access as for in vivo acquisitions due to its small size compared to the available space makes the use of solenoid geometries a good choice of coil design. Solenoid coils can naturally produce a highly homogeneous and efficient B_1 field perpendicular to the main magnetic field if the coil axis is perpendicular to the B_0 field. For MRI applications, other well-known coil designs such as saddle coil [13], alderman grant resonator [14] and birdcage coils [15] are often used to produce a homogenous B_1 field during excitation. These designs are known as transverse resonators, with a cosine-dependent current distribution flowing parallel to the cylindrical axis [12]. When the current distribution produces RF field along their symmetry axis, they are called axial resonators, which include geometries such as the solenoid [16] and the loop-gap resonator [17]. Several studies have reported the use of solenoid designs for *ex vivo* MRI in low- and mid-field strength [9,16] with applications such as animal imaging in clinical scanners [18,19], and microscopic MRI. At UHF, the challenge in developing volume RF coils is the strong interaction due to electrical coupling between electrically conductive samples and the coil conductors, particularly when the electrical length approaches the wavelength of the RF signal at the Larmor frequency. Furthermore, for solenoidal RF coil designs, the structure might become self-resonant at frequencies below the Larmor frequency, depending on the electrical length of the conductor. An alternative to avoid strong interactions between sample and conductors is the segmentation of the solenoid turns with fixed tuning capacitors, which will increase the total capacitive reactance of the coil and, consequently, decrease the effect of stray capacitances in the coil structure.

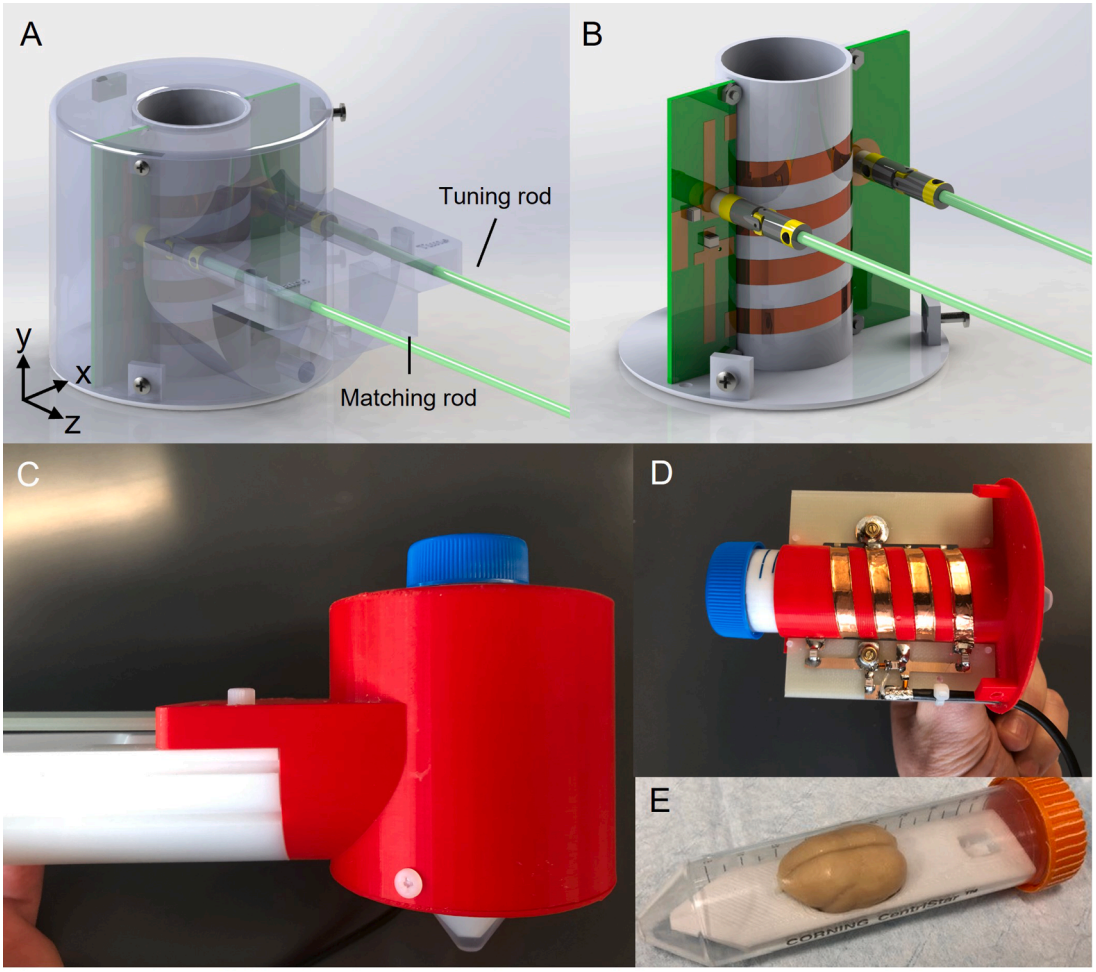

Fig. 3. (A and B) Rendered 3D pictures of the computer aided design file in perspective view showing the 400 MHz solenoid designed to maximize the filling factor of marmoset brain samples conditioned in 50 mL conical centrifuge tubes. (C) Side view of the coil attached to the BRUKER mouse cradle. (D) Photo of the 400 MHz solenoid build. (E) Typical marmoset brain sample conditioned in a 50 mL conical centrifuge tube.

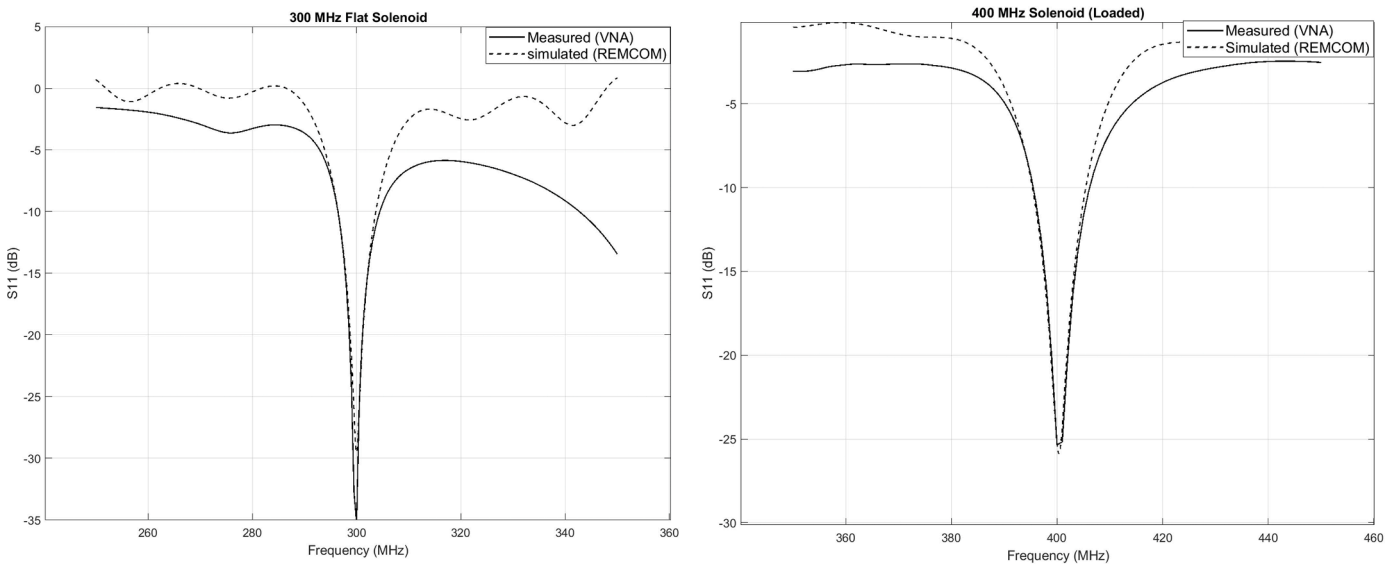

Fig. 4. S_{11} responses obtained from the REMCOM XFdtd simulations (dotted lines) and from measurements with VNA (solid lines) obtained with the loaded 300 MHz solenoid (left) and with the loaded 400 MHz solenoid (right).

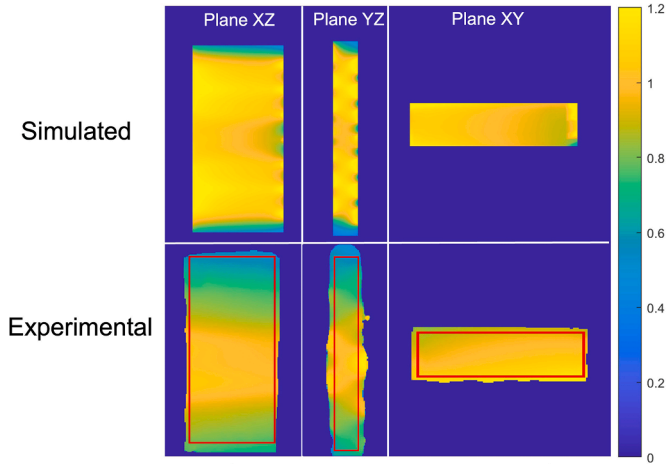

Fig. 5. Simulated and experimental B_1^+ maps obtained from the three principal planes (according to the coordinate system of Fig. 1A) for the 300 MHz flat solenoid loaded. For the experimental B_1^+ maps, the Non-Uniformity was calculated inside the ROIs defined by the red lines.

Two RF coils operating as transmitter/receiver based on the solenoid geometry were built: one coil for *ex vivo* MRI of human brain tissues at a clinical whole-body 7T scanner (MAGNETON 7T, SIEMENS, Erlangen, Germany) located at the School of Medicine of the University of Sao Paulo (Brazil); and another coil for ex vivo MRI of marmoset brain samples at a 9.4T preclinical scanner (Bruker-Biospin, Inc, Ettlingen, Germany), located at the Department of Neurobiology, at University of Pittsburgh (USA). The solenoid for 7T *ex vivo* MRI (referred to here as the 300 MHz flat solenoid) was designed to maximize the filling factor for human brain tissues conditioned in histology processing cassettes (Leica Biosystems, IL, USA) made of acetyl polymer and measuring 40 mm long x 30 mm width x 6 mm thick. According to the definition given in the introduction by Eq. (1), the estimated filling factor considering a typical ex vivo brain sample, as shown in Fig. 1E, is $\eta_{FlatSolenoid} \approx 0.1$. It is important to emphasize that the histological cassettes where the samples are conditioned occupy extra space inside the coil volume. As a comparison, the estimated filling factor for the commercial 7T head coil available is $\eta_{7T\ Head\ coil} \approx 8.9 \times 10^{-4}$. All the 3D files for the 300 MHz flat solenoid were designed using SolidWorks 2022 (Dassault Systèmes) for 3D printing using PLA, as shown in Fig. 1A.

The 300 MHz flat solenoid coil was designed with seven turns of 6.3 mm width copper tape (3 M) spaced by 7.8 mm on a 3D printed support using PLA plastic. Non-magnetic 2.4 pF capacitors (0505 series 500 V, Passive Plus) were inserted halfway of each turn on the opposite side of the tune-and-match circuit, decreasing the total electrical length of the solenoid and increasing the capacitive reactance of the coil at 300 MHz. This modification made it less sensitive to stray capacitances, consequently decreasing dielectric coupling with the sample when the coil was loaded. To allow fine tuning at 300 MHz and matching at 50 Ω prior to each acquisition, variable non-magnetic trimmers (5 pF – 30 pF, 2 kV, Voltronics) were inserted in parallel, as indicated in the coil schematic of Fig. 1-B. A 50Ω RG-316 coaxial cable with a non-magnetic BNC connector was directly soldered to the coil PCB through a balanced λ/4 lattice balun [11]. Round garolite rods (6 mm OD, 1.6 wall thickness) were used as guide tubes to allow the fine-tuning and matching adjustments of the non-magnetic trimmers with tuning rods prior to each scan using a RF frequency Sweeper (505NV+ Morris Instrument Inc, Ottawa, Canada). No RF shielding was used for this coil since the gradient coil in this whole-body scanner is located far enough from the RF coil. Since this coil operates as a transmitter/receiver (T/R), a 300 MHz T/R switch (Stark Contrast MRI Coils Research, Erlangen, Germany) was necessary to interface the coil with the MRI scanner. The T/R switches [20] protect the low-noise preamplifier from high RF power during transmission using active circuits with PIN diodes inserted into the path between transmit and receive ports, avoiding the noise from being coupled from the transmit port to the preamplifier in receive mode. Fig. 2 shows the linear SIEMENS 7T TR switch used, with a non-magnetic BNC connector soldered directly into the PCB input. The output was connected to a 7T Tim Tx/8Rx cable Assembly (SIEMENS) terminated with ODU plugs and assembled inside a plastic box, which can be used as an interface box for different designs of homebuilt RF coils.

The second RF solenoid coil built, also operating as transmitter/receiver, was designed to perform ex vivo MRI at 9.4T (Larmor frequency of ^{1}H at 9.4T is 400 MHz) in a preclinical small-bore scanner (9.4T/30 cm USR magnet, BRUKER, Biospec) for high spatial resolution MRI acquisition of ex vivo marmoset brain samples placed in polypropylene centrifuge tubes (50 mL, Thermofisher), with an outer diameter of 30 mm. For the 400 MHz solenoid, marmoset brain samples are placed in 50 ml centrifuge tubes (measuring approximately 28 mm

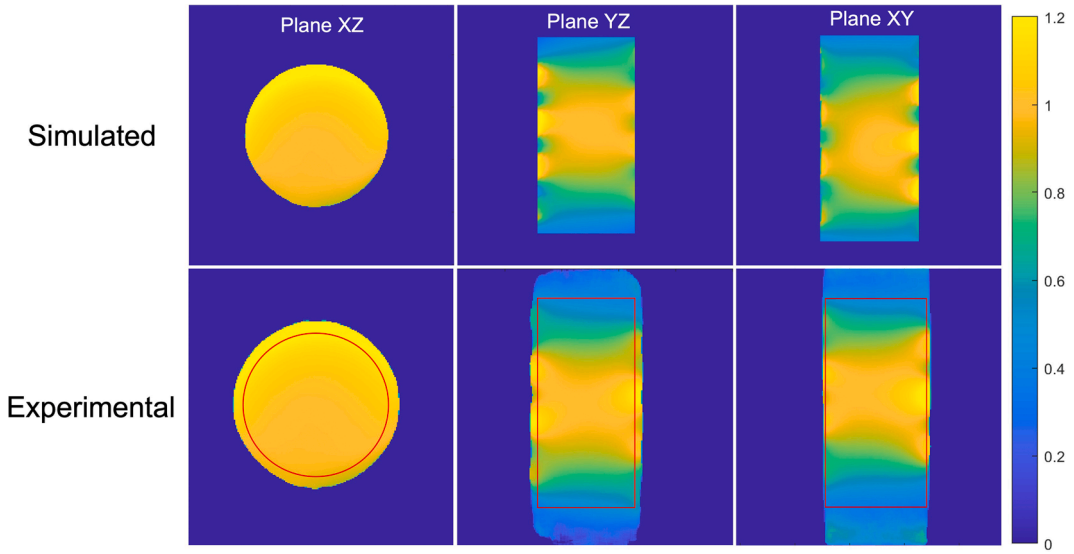

Fig. 6. Simulated and experimental B_1^+ maps obtained from the three principal planes (according to the coordinate system of Fig. 3A) for the 400 MHz solenoid loaded. For the experimental B_1^+ maps, the non-uniformity was calculated inside the ROIs defined by the red lines.

Table 1
Non-uniformity values obtained from the simulated and measured B_1^+ maps from Fig. 5 and Fig. 6.

	300 MHz Flat Solenoid		400 MHz solenoid	
	Simulated	Experimental	Simulated	Experimental
NU_{XY}	7.8%	8.7%	8.5%	7.8%
NU_{XZ}	10.8%	13.5%	24.4%	26.4%
NU_{YZ}	14.1%	17.3%	22.7%	25.7%

diameter x 90 mm long). The estimated filling factor is $\eta_{400MHz\ Solenoid} \approx 0.36$. It is essential to note that the samples must be placed inside specialized containers occupying space in the coil. The rendered 3D files of this coil were also designed in SolidWorks and are shown in Fig. 3A and Fig. 3B. The cover of the coil was designed so that it was possible to attach it to a commercial Bruker mouse cradle (Fig. 3C), which manually slides into the isocenter of the 9.4T magnet. The cover and support of this coil were 3D printed using PLA plastic, with thumb M5 nylon screws to attach the coil to the mouse cradle. This solenoid was built using 6 mm width copper tape (3 M) with four 29 mm inner diameter turns spaced by 5 mm. For each turn, a gap of 1 mm was inserted in the copper tape with 1.8 pF capacitors (Non-magnetic 0505 series 500 V, Passive Plus, Huntington, USA) soldered, making the solenoid coil resonant at 400 MHz. The same balanced matching network consisting of $\lambda/4$ lattice balun was used to linearly drive the coil with an RG-316 coaxial cable directly soldered in the PCB, as seen in Fig. 3D. Variable non-magnetic trimmers (Knowles-Voltronics) with extended shafts connected to 1.8 m long G10 rods through universal plastic joints (Chemical-Resistant U-Joint for 1/8″ diameter, McMASTER-CARR) were used to allow fine-tuning and matching when the coil is loaded with the marmoset brain sample and positioned at the isocenter of the magnet. For this 9.4T preclinical scanner, the verification of tuning/matching was performed directly on a built-in screen at the back of the 9.4T magnet. No RF shield was used for this coil as well.

A 3D-printed brain holder was designed to fit inside the tubes to hold the brain sample centered at the 50 mL tubes (Fig. 3E), holding the samples immersed in Fomblin oil (Solvay USA, Inc.) during the acquisitions.

Both RF coils were characterized on the workbench using a Vector Network Analyzer (VNA, ZNL3, Rhodes & Schwarz, Columbia, MD, USA). The coil losses were evaluated by measurement of the quality factor (Q, [21]) when the solenoid coils were loaded (Q_L) and unloaded (Q_U). The Q is determined as the ratio between the center frequency and the bandwidth at −3 dB of the S_{21} response curve using a pair of decoupled pickup loops. Both coils' reflection coefficients (S_{11}) were measured when the coil was loaded and directly connected to the VNA port-1.

Electromagnetic simulations were performed to evaluate the B_1^+ distribution produced by both solenoid designs using finite-difference time-domain software (REMCOM XFdtd, State College, PA, USA). The coils were simulated in linear polarization loaded with a phantom filled with tissue-simulating liquid [22,23] ($\sigma = 0.8$ S/m and $\varepsilon_r = 43.6$). The capacitors' equivalent series resistance (ESR) was estimated at 0.1Ω, according to the datasheet provided by the capacitor's manufacturer (Passive Plus, Huntington, USA). The 300 MHz flat solenoid was simulated assuming a capacitance of 2.2 pF, while the value used in the constructed coil was 2.4 pF (8% difference between simulation and experiment). For the 400 MHz solenoid, the coil was simulated with 1.9 pF capacitors, while the coil was built using 1.8 pF (5% difference). The feeding ports were modeled as 50 Ohms components. The resistance of the copper conductors considered the skin depth effects at the simulated frequencies (300 MHz and 400 MHz) [24]. For the 300 MHZ flat solenoid simulations, the number of meshes for plane XY was 39, 136 for plane XZ, and 54 for plane YZ, resulting in a total computing time of 1 min and 32 s. The 400 MHz solenoid was simulated with 47 meshes for plane XY, 66 for plane XZ, and 54 for plane YZ, with a total computing time of 1 min and 7 s. The different number of mesh cells is because the software REMCOM XFdtd uses a tool called Project Optimized Gridding (Progrid), which varies the number and size of the cells in each direction, depending on the geometry. All simulations were performed on a desktop computer (Intel Core i5–10400F CPU, 6 cores, 12 threads, 2.91 GHz with 32GB DDR3 RAM and Nvidia GeForce GTX 1050 graphic card (4GB GDDR5 RAM)) running a 64-bit Windows 8 operation system.

Both coils were characterized in their respective scanners, i.e., the 300 MHz solenoid at the whole body 7T clinical scanner (SIEMENS) and the 400 MHz solenoid in the 9.4T preclinical scanner (BRUKER), using a cassette and a conical centrifuge tube, respectively, filled with $CuSO_4$ $5H_2O$ (1 g/L) and NaCl (3.6 g/L) solution. Experimental B_1^+ field maps were obtained using the Double Angle Method [25]. Field homogeneity was evaluated by calculating the parameter known as Non-Uniformity (NU), defined as the ratio (Standard Deviation)/Average of the pixels inside a region-of-interest (ROI) encompassing approximately 80% of the phantom cross-sectional area [26].

The 300 MHz flat solenoid was tested in the 7T clinical scanner

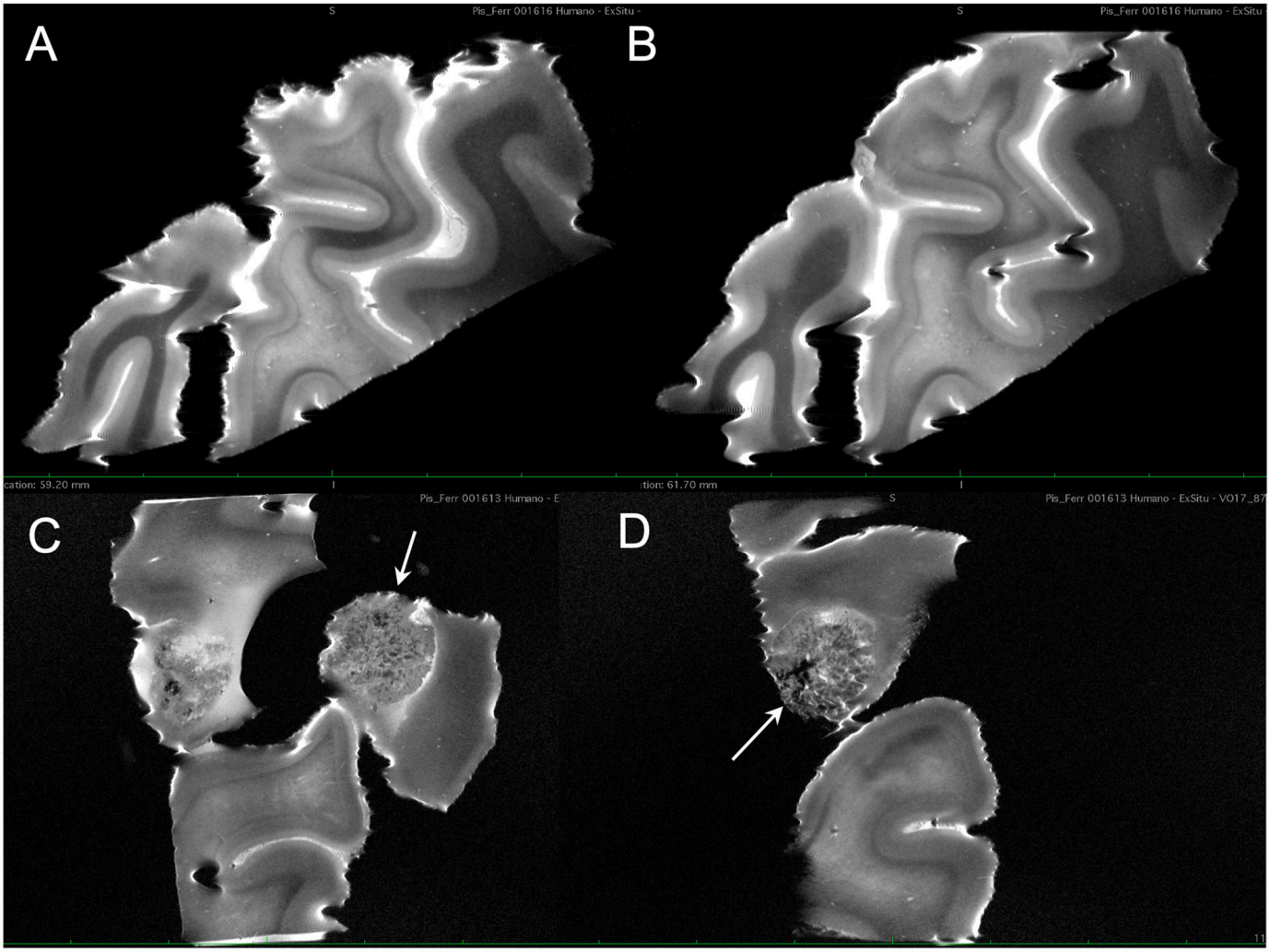

Fig. 7. A, B, C, and D show different slices of *ex vivo* MRI acquired from human brain samples (as seen in Fig. 1E) using the 300 MHz flat solenoid in a 7T whole-body clinical scanner. Images were acquired with 80 μm in-plane resolution and 500 μm slice thickness, which allows the identification of different cortical layers. Images C and D show the presence of highly heterogeneous neoplastic lesions (arrows).

interfaced with the T/R switch shown in Fig. 2. T2-weighted images were acquired from brain samples conditioned in histology cassettes (as seen in Fig. 1E) using a Turbo Spin-Echo pulse sequence, with slice thickness=500 μm, TR/TE = 5000/45 ms, FOV_{phase}/FOV_{read} = 95/47 mm, N_{phase}/N_{read} = 1200/600, 1 Average, with a total acquisition time of 50 min. The SNR of the ex vivo brain samples was measured from images acquired with the 300 MHz flat solenoid and compared against the commercially available 7T head coil. The signal is calculated as the mean value of an ROI defined in the sample and the noise as the standard deviation of an ROI defined in the background noise.

The 400 MHz solenoid was tested in a preclinical 9.4 T scanner with the acquisition of 60 μm isotropic images using a fast low angle shot (FLASH) 3D sequence, TR/TE = 100/20 ms, Flip Angle = 52,6°, FOV = 35 × 25 × 20 mm, matrix size of 700 × 500 × 400 and 1 average, resulting in a total acquisition time of 5 h 33 min.

3. Results

The Q measurements ratio obtained for the 300 MHz flat solenoid performed on the workbench resulted in $Q_U/Q_L = 106/42 = 2.5$. For the 400 MHz solenoid, the Q ratio measurements resulted in Q_U/Q_L=262/154=1.7. The S_{11} responses obtained through simulations with REMCOM XFdtd and from the VNA measurements are shown in Fig. 4. These workbench measurements show that both coils can be perfectly tuned and matched to 50Ω at the Larmor frequency under different loading conditions. It is important to mention that a good matching (i.e., S_{11} better than −30 dB) could always be achieved by adjusting the tuning and matching trimmers, maximizing the coil efficiency during transmission and the SNR before each acquisition.

Fig. 5 shows the B_1^+ maps obtained from electromagnetic simulations and the flip angle maps obtained for the 300 MHz flat solenoid for the three principal planes, according to the reference system from Fig. 1. The B_1^+ maps were normalized by the value at the coil isocenter to allow direct comparison between simulation and experiments. The ROIs marked in red in the experimental B_1^+ maps are used to calculate the non-uniformity parameter.

Fig. 6 shows the simulated and measured B_1^+ maps obtained for the 400 MHz solenoid at the three primary planes, according to the reference system from Fig. 3. Again, all B_1^+ maps were normalized by the value at the coil isocenter, and the NU was calculated inside the ROIs marked in red.

The NU values were calculated from the simulated and experimental B_1^+ maps and are summarized in Table 1.

Fig. 7 shows the ex vivo T_2-weighted images with 80 μm in-plane resolution and 500 μm slice thickness acquired from human brain samples (as seen in Fig. 3E) using the 300 MHz flat solenoid at the 7T clinical MRI scanner.

Compared to the commercially available 7T head coil, the SNR

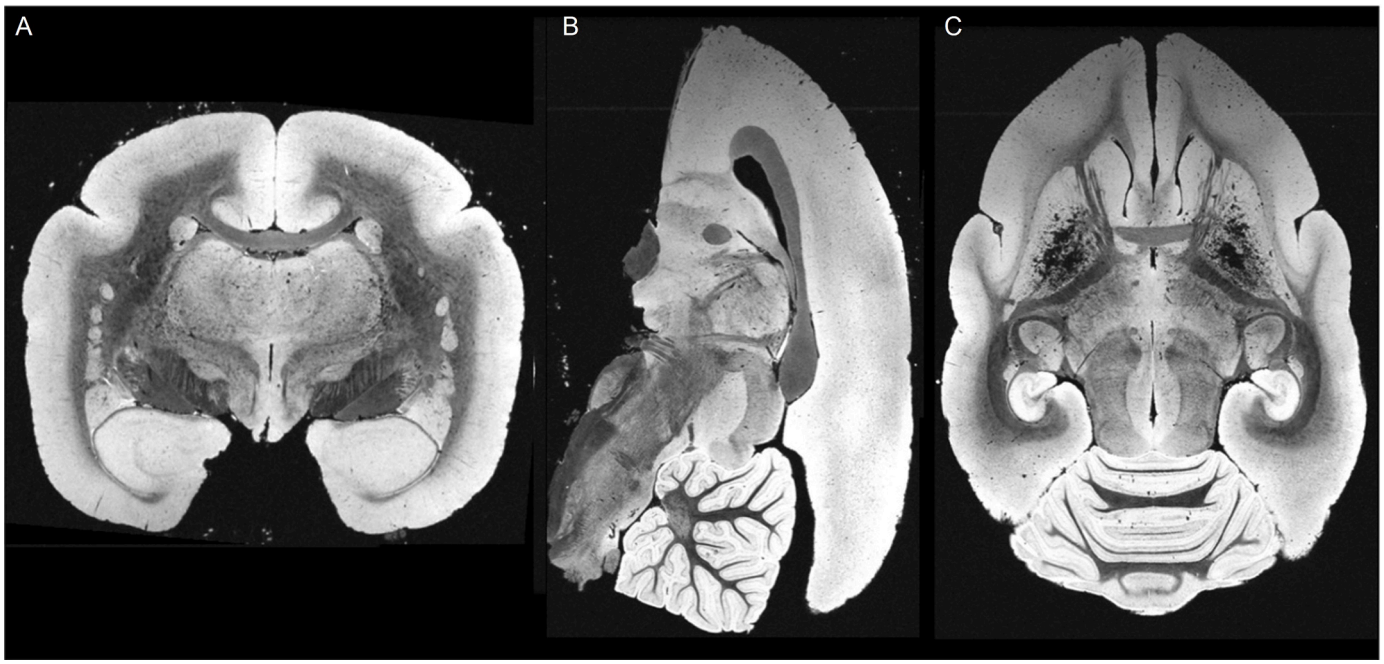

Fig. 8. T_2* weighted ex vivo images from a marmoset brain immersed in Fomblin oil acquired with 60 μm isotropic resolution using the 400 MHz solenoid. A) Coronal. (B) Sagittal. C) Axial.

measurements from the same ex vivo brain sample images acquired with the 300 MHz flat solenoid achieved 11 times higher SNR. However, it is important to note that we are comparing a dedicated ex vivo solenoid coil with a much higher filling factor with a volume coil loaded with a very small sample.

Fig. 8 shows T_2*-weighted 60 μm isotropic resolution images acquired from a marmoset brain sample using the 400 MHz solenoid in a 9.4T preclinical scanner.

4. Discussion

This paper describes the development and characterization of two RF coil designs based on the solenoid geometry with a high filling factor: one optimized for *ex vivo* MRI of brain tissue samples at 7T clinical scanner; the second geometry was optimized for *ex vivo* MRI of marmoset brain samples at a 9.4T preclinical small bore animal scanner. Although both solenoid coils were designed with optimized filling factors, the Q factor measurements performed on the workbench with the coils in the loaded and unloaded conditions have shown that the primary noise source is likely to be in the sample losses-dominated regime. The losses due to the antenna effect and coupling with the sample through electric fields could be minimized by the insertion of capacitors in each turn of the solenoid geometry, allowing the tuning and matching in the loaded condition to be performed. The reflection coefficient (S_{11}) measured on the workbench for both coil designs was verified to be better than −25 dB. Since both coils were used as transmitter/receiver, the good 50Ω matching minimized the excitation power during transmission, with maximized SNR for receiving. The simulated B_1^+ maps of both geometries showed a good correlation with experimental flip-angle maps obtained from phantoms by the Double Angle Method. Although the B_1^+ maps obtained for the 300 MHz flat solenoid showed an attenuation near the edges in the XZ and YZ orientation, no signal loss was observed in the *ex vivo* images acquired from the human brain tissue samples shown in Fig. 7. One possible explanation for the differences observed between the simulated and the experimental $B1^+$ maps, which are noticeable for the 300 MHz flat solenoid (Planes XZ and YZ from Fig. 5), are due to differences in the conductivity and relativity permittivity values used to model the phantom material. Although we used conductivity and relative permittivity values commonly reported [22,23] for phantom simulations (i.e., $\sigma = 0.8$ S/m and $\varepsilon_r = 43.6$), the phantom solution (CuSO4 5H2O (1 g/L) and NaCl (3.6 g/L)) used in the VNA measurements may have different values. Nevertheless, ex vivo images acquired with the 300 MHz flat solenoid allowed the acquisition of T2W images with 80 μm in-plane resolution and 500 μm slice thickness of human brain tissues in a 7T whole-body clinical scanner. Due to its intrinsically low filling factor, such high resolution cannot be achieved with high SNR for small samples using the commercially available coils for 7T whole-body scanners. Even for the preclinical 9.4T scanner, the 400 MHz solenoid allowed the images from a marmoset brain sample to be acquired with 60 μm isotropic resolution. Although this resolution can be achieved using commercially available RF coil designs for preclinical scanners, such as millipede volume coils [27], the transmit/receive solenoid coil described here represents a simple choice for high-resolution MRI of ex vivo samples.

5. Conclusion

The high homogeneity achieved during excitation obtained at the volume of interest for both coil designs, as verified by the B_1^+ experimental maps and from NU values, as well as the high-resolution *ex vivo* images obtained with high SNR, confirm the use of solenoid coils as a simple, affordable, and efficient alternative for MRI of ex vivo brain samples at UHF.

Declaration of Competing Interest

The authors declare that they have no known competing financial interests or personal relationships that could have appeared to influence the work reported in this paper.

Data availability

Data will be made available on request.

Acknowledgments

This work was supported by the Pennsylvania Department of Health [SAP# 4100083102]; the National Institute on Aging [grant numbers R24AG073190, U19AG074866]; and São Paulo Research Foundation [grant number 2009/54323–0].

References

[1] A. Pfefferbaum, E.v. Sullivan, E. Adalsteinsson, T. Garrick, C. Harper, Postmortem MR imaging of formalin-fixed human brain, Neuroimage (2004), https://doi.org/10.1016/j.neuroimage.2003.11.024.
[2] R.J. Dawe, D.A. Bennett, J.A. Schneider, S.K. Vasireddi, K. Arfanakis, Postmortem MRI of human brain hemispheres: t 2 relaxation times during formaldehyde fixation, Magn. Reson. Med. (2009), https://doi.org/10.1002/mrm.21909.
[3] B.L. Edlow, et al., 7 Tesla MRI of the ex vivo human brain at 100 μm resolution, Sci. Data (2019), https://doi.org/10.1038/s41597-019-0254-8.
[4] K. Schmierer, et al., Diffusion tensor imaging of post mortem multiple sclerosis brain, Neuroimage (2007), https://doi.org/10.1016/j.neuroimage.2006.12.010.
[5] C. Langkammer, et al., Quantitative susceptibility mapping (QSM) as a means to measure brain iron? A post mortem validation study, Neuroimage 62 (3) (2012), https://doi.org/10.1016/j.neuroimage.2012.05.049.
[6] A. Roebroeck, K.L. Miller, M. Aggarwal, Ex vivo diffusion MRI of the human brain: technical challenges and recent advances, NMR Biomed. (2019), https://doi.org/10.1002/nbm.3941.
[7] A.S. Shatil, K.M. Matsuda, C.R. Figley, A method for whole brain ex vivo magnetic resonance imaging with minimal susceptibility artifacts, Front. Neurol. 7 (NOV) (2016), https://doi.org/10.3389/fneur.2016.00208.
[8] D.I. Hoult, R.E. Richards, The signal-to-noise ratio of the nuclear magnetic resonance experiment, J. Magn. Reson. 24 (1) (1969) 1976, https://doi.org/10.1016/0022-2364(76)90233-X.
[9] D.M. Hoang, E.B. Voura, C. Zhang, L. Fakri-Bouchet, Y.Z. Wadghiri, Evaluation of coils for imaging histological slides: signal-to-noise ratio and filling factor, Magn. Reson. Med. 71 (5) (2014), https://doi.org/10.1002/mrm.24841.
[10] P.B. Roemer, W.A. Edelstein, C.E. Hayes, S.P. Souza, O.M. Mueller, The NMR phased array, Magn. Reson. Med. (1990), https://doi.org/10.1002/mrm.1910160203.
[11] J. Mispelter, M. Lupu, A. Briguet, NMR Probeheads for Biophys. Biomed. Experiments (2015), https://doi.org/10.1142/p759.
[12] J. Mispelter, M. Lupu, Homogeneous resonators for magnetic resonance: a review, Comptes. Rendus Chimie 11 (4–5) (2008), https://doi.org/10.1016/j.crci.2007.10.003.
[13] J.W. Carlson, Currents and fields of thin conductors in rf saddle coils, Magn. Reson. Med. 3 (5) (1986), https://doi.org/10.1002/mrm.1910030513.
[14] D.W. Alderman, D.M. Grant, An efficient decoupler coil design which reduces heating in conductive samples in superconducting spectrometers, J. Magn. Reson. 36 (3) (1969) 1979, https://doi.org/10.1016/0022-2364(79)90123-9.
[15] C.E. Hayes, W.A. Edelstein, J.F. Schenck, O.M. Mueller, M. Eash, An efficient, highly homogeneous radiofrequency coil for whole-body NMR imaging at 1.5 T, J. Magn. Reson. (1969) (1985), https://doi.org/10.1016/0022-2364(85)90257-4.
[16] V. Vegh, P. Gläser, D. Maillet, G.J. Cowin, D.C. Reutens, High-field magnetic resonance imaging using solenoid radiofrequency coils, Magn. Reson Imaging 30 (8) (2012), https://doi.org/10.1016/j.mri.2012.04.027.
[17] J.P. Hornak, T.L. Ceckler, R.G. Bryant, Phosphorus-31 NMR spectroscopy using a loop-gap resonator, J. Magn. Reson. 68 (2) (1969) 1986, https://doi.org/10.1016/0022-2364(86)90248-9.
[18] S.S. Hidalgo, D. Jirak, S.E. Solis, A.O. Rodriguez, Solenoid coil for mouse-model MRI with a clinical 3-Tesla imager: body imaging, Revista Mexicana de Fisica 55 (2) (2009).
[19] H.S. Lee, D.C. Woo, K.H. Min, Y.K. Kim, H.K. Lee, B.Y. Choe, Development of a solenoid RF coil for animal imaging in 3 T high-magnetic-field MRI, Scanning 30 (5) (2008), https://doi.org/10.1002/sca.20118.
[20] B. Thapa, J. Kaggie, N. Sapkota, D. Frank, E.K. Jeong, Design and development of a general-purpose transmit/receive (T/R) switch for 3T MRI, compatible for a linear, quadrature and double-tuned RF coil, Concepts Magn. Reson. Part B Magn. Reson. Eng. (2016), https://doi.org/10.1002/cmr.b.21321.
[21] A. Haase, et al., NMR probeheads for in vivo applications, Concepts Magn. Reson. 12 (6) (2000) 361–388, doi: 10.1002/1099-0534(2000)12:6<361::AID−CMR1>3.0.CO;2-L.
[22] S. Orzada, A novel 7 T microstrip element using meanders to enhance decoupling,", Magn. Reson. Med. : Official J. Soc. Magn. Reson. Med. /Soc. Magn. Reson. Med. 14 (2008).
[23] S. Orzada, et al., A 32-channel parallel transmit system add-on for 7T MRI, PLoS ONE 14 (9) (2019), https://doi.org/10.1371/journal.pone.0222452.
[24] G. Giovannetti, V. Hartwig, L. Landini, M.F. Santarelli, Classical and lateral skin effect contributions estimation in strip MR coils, Concepts Magn. Reson. Part B Magn. Reson. Eng. 41 B (2) (2012), https://doi.org/10.1002/cmr.b.21210.
[25] R. Stollberger, P. Wach, Imaging of the active B1 field in vivo, Magn. Reson. Med. 35 (2) (1996), https://doi.org/10.1002/mrm.1910350217.
[26] C.E.G. Salmon, E.L.G. Vidoto, M.J. Martins, A. Tannús, Optimization of saddle coils for magnetic resonance imaging, Brazilian J. Phys. (2006), https://doi.org/10.1590/S0103-97332006000100004.
[27] (Ernest) W.H. Wong, Millipede Coils. Encyclopedia of Magnetic Resonance, 2011, https://doi.org/10.1002/9780470034590.emrstm1133.